Benguela Dynamics
Pillar, S. C., Moloney, C. L., Payne, A. I. L. and F. A. Shillington (Eds). *S. Afr. J. mar. Sci. 19: 61–73*
1998

THE PHYSICAL STRUCTURE OF AN UPWELLING FILAMENT OFF THE NORTH-WEST AFRICAN COAST DURING AUGUST 1993

E. NAVARRO-PÉREZ and E. D. BARTON**

Recent work in the Canary Current upwelling system highlights the role of previously uninvestigated filament structures. A filament located near 27°N in summer 1993 extended 150 km offshore with a width of ~20 km and surface temperature anomaly up to 2°C. The cool temperature signal was restricted to a shallow surface layer, and the filament was entrained around a large cyclonic eddy. Offshore transport in the filament, in excess of 1 Sv, may be a major influence in dispersal of material originating in the region of active coastal upwelling. The location of the filament studied appears repeatable from year to year, suggestive of a strong relation with the topographically trapped eddy, which was situated downstream of a lateral ridge between the Canary Islands and the African coast.

Upwelling filaments are cold, typically narrow features in surface temperature extending hundreds of kilometres offshore from a coastal upwelling zone (Flament *et al*. 1985). They are defined by strong lateral temperature gradients, are associated with strong offshore flows and often terminate in eddy-like structures (Kosro and Huyer 1986). Furthermore, filament waters are typically rich in nutrients and high in chlorophyll because of their origin in the nearshore upwelling. As filament waters are advected offshore, their values of sea surface temperature and chlorophyll approach those of the open ocean (Van Camp *et al.* 1991). The importance of their role in exchanges between the continental shelf and the open ocean is not well known.

Filament structures have been documented off the coasts off California (Brink and Cowles 1991), Portugal (Haynes *et al*. 1993) and south-western Africa (Lutjeharms and Stockton 1987). Flament *et al*. (1985) and Huyer *et al.* (1991) reported the presence of a distinct filament core containing fresher and cooler water which separated different water masses to either side of the structure. This they interpreted as evidence that the filament waters were upwelled at the coast upstream of the area and not locally.

Filament formation has been investigated in numerous modelling studies. Ikeda and Emery (1984) introduced the idea that filaments could be related to meanders or eddies induced by instabilities of an idealized California Current. Pierce *et al.* (1991) studied stability with a linear six-layer quasi-geostrophic model initiated with observed velocity profiles. McCreary *et al*. (1991), using a $2\frac{1}{2}$ layer numerical model with uniform wind and regular topography, concluded that, after development, seasonal upwelling fronts and jets eventually become unstable and move offshore, developing into meandering jets and eddy fields. Allen *et al.* (1991) and Haidvogel *et al.* (1991) pursued the question of current stability in greater detail, the latter using a primitive-equation model allowing more realistic approximations. Their results indicate that a minimum of four physical factors is necessary to produce the phenomenologically realistic filaments observed in the coastal transition zones. These are a forced equatorward flow at the surface (generally forced by the wind, but possibly a consequence of the larger-scale ocean circulation), a source of cold water along the coast (in general a result of active upwelling) bottom topography of finite amplitude, and an irregular coastline geometry.

Another possible physical cause for the formation of cold filaments is the interaction of coastal upwelled water with a pre-existing offshore eddy field (Mooers and Robinson 1984, Rienecker and Mooers 1989). The coupled effect of cyclonic and anticyclonic mesoscale eddies could draw the recently upwelled water seawards, producing surface temperature signatures comparable to observed filaments. The effects of wind-stress curl were investigated by Narimousa and Maxworthy (1986) in laboratory tank experiments. They showed the formation of offshore migrating eddies that had an important role in the offshore transport of the upwelled water.

Strub *et al.* (1991) proposed three conceptual models of the formation of filaments. The first was that filaments are the results of "squirts" or one-way jets, transporting coastally upwelled water to the deep ocean, and sometimes terminating in a counter-rotating vortex pair. The resulting "mushroom," "hammerhead," or "T" shapes in sea surface temperature and pigment

* School of Ocean Sciences, University of Wales (Bangor), Menai Bridge, Anglesey LL59 5EY, United Kingdom. Email: oss021@bangor.ac.uk
Manuscript received: January 1997

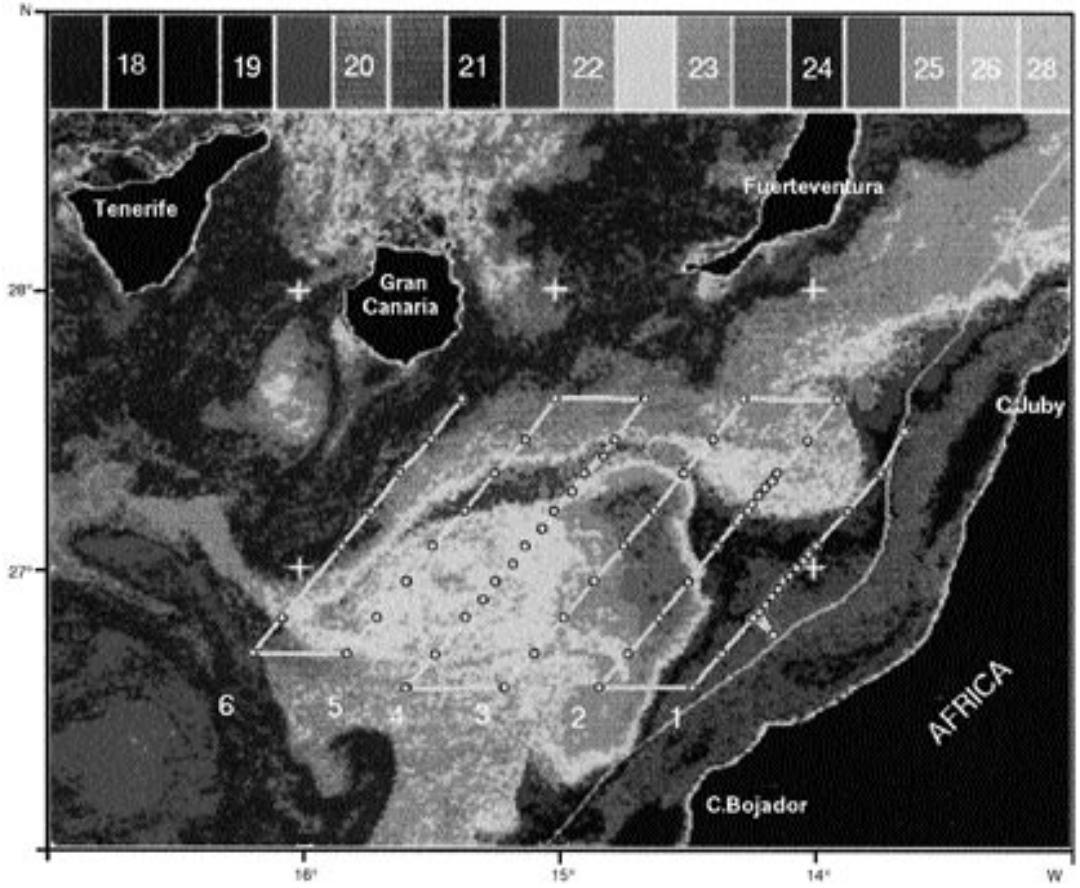

Fig. 1: Sea surface temperature image for 10 August 1993. Survey station transects and the 200 m isobath are shown. Coastal upwelling over the shelf extends seaward in a narrow filament north of Cabo Bojador. A cold-core eddy is evident south-west of Gran Canaria, south of which there is a warm lee

fields were described by Ikeda and Emery (1984). A squirt is generated by nearshore convergence, caused by local wind relaxation around capes (Kosro and Huyer 1986), or other mechanism. The second model consisted of a number of mesoscale eddies imbedded in a slow equatorward current (Mooers and Robinson 1984). Where eddies draw recently upwelled water away from the coast, they create a surface temperature structure similar to a squirt. The last conceptual model consisted of a continuous equatorward jet, meandering offshore and onshore. During onshore excursions, the jet entrains coastally upwelled water and creates filaments of cold, rich water which extend offshore on the next meander. Closed eddies may be created on either side of the jet by instabilities of the flow, but water in the core of the meandering jet may originate from far upstream, which would not be the case for a squirt and would occur only haphazardly in a mesoscale eddy field.

Filaments in the Canary Current region off North-West Africa have been reported from Advanced Very High Resolution Radiometer (AVHRR) observations of sea surface temperature and Coastal Zone Colour Scanner (CZCS) observations of chlorophyll-like pigment concentration (Hernández-Guerra 1990, Van Camp *et al*. 1991). However, no information on their subsurface structure was available. In August 1993 a cruise took place in the Canary Island region to study an upwelling filament located between Cabo Juby and Cabo Bojador. *In situ* measurements of the hydrographic and velocity structure were obtained for the first time in a North-West African filament.

Questions addressed included:

(i) What is the structure of the filament? What is the nature of its boundaries? What depth range does it occupy? What is its maximum offshore extent?
(ii) What is the related velocity structure of the filament? Is there a resultant significant offshore transport?
(iii) On the larger scale, what is the origin of this filament? Is it part of a meander of the Canary Current, is it a "squirt" produced locally, or is it produced by an offshore eddy field?

The results herein provide a kinematic description of an upwelling filament off North-West Africa. Filaments may make a significant contribution towards the important process of exchanges between coastal waters and the open ocean, which are poorly understood. This work forms part of a wider study of variability in the Canary Current (Navarro-Pérez 1996).

DATA AND METHODS

The sampling plan was based on prior knowledge of the area obtained with AVHRR sea surface temperature imagery. A dense grid of stations was sampled over a period of six days along six transects parallel to the African coast. The nominal station separation was 20 km, although many additional stations were inserted across filament boundaries (Fig. 1). Near-surface conditions were sampled continuously with the ship's thermosalinometer. The transects were numbered in order of distance from the African coast. Transect 1 was located close to the main upwelling front situated over the edge of the continental shelf (about 200 m depth). The other transects covered a region extending roughly 160 km alongshore and 200 km offshore, extending to the longitude of the island of Gran Canaria.

The CTD measurements were made with a Sea-Bird Electronics SBE-911 Plus model at a lowering rate of approximately 1 $m \cdot s^{-1}$. The casts were made from the surface to 1 000 m at most stations, although the additional casts were generally limited to 300 m. Details of data processing are reported by Navarro-Pérez *et al.* (1994). The continuous near-surface data obtained with the thermosalinometer were recorded at time intervals of 1 minute (Pacheco and Hernández-Guerra 1995).

Acoustic Doppler Current Profiler (ADCP) and continuous Global Positioning System (GPS) measurements were made to determine absolute velocities in the upper 400 m. Current profiles were acquired during the cruise from an RDI ADCP operating at a frequency of 150 kHz. Data were collected in 8-m vertical bins to a maximum depth of 400 m, excluding any data with the Percent Good below 30%. The transducer was mounted roughly amidship, 4 m below the waterline. The first bin was blanked and the shallowest accepted bin was from 16 to 24 m. The relative velocities from each ping (1 per second) were averaged and combined with GPS data to provide absolute velocity estimates at 5-minute intervals. Tidal currents in the region are considered to be small (Huthnance and Baines 1982). Estimates of semi-diurnal tides from the ADCP data indicated flows of <0.08 $m \cdot s^{-1}$ orientated north-east to south-west and so no removal of tides was made. More detailed discussion of the ADCP data processing is given by Navarro-Pérez and Barton (1995).

RESULTS

Surface structure

The cruise was carried out in early August 1993 at the peak of the trade-wind season. Throughout the period, winds blew consistently and strongly from the north-east. Immediately prior to the filament survey, winds exceeded 20 $m \cdot s^{-1}$ for several days, but then moderated to values of about 10 $m \cdot s^{-1}$ for the rest of the cruise. The oceanographic situation during the survey is depicted in a satellite SST image from 10 August 1993 (Fig. 1), in which a variety of mesoscale features are apparent. Among these are warm island-lee regions and island-related eddies, both studied during the cruise and reported elsewhere (Barton *et al.* in press). Coastal upwelling along the African coast is seen clearly extending slightly beyond the 200 m depth contour. The strongest upwelling and coldest waters were inshore, south of capes.

Between Cabo Juby and Cabo Bojador, a filament was evident as a major contortion of the upwelling front separating nearshore cool upwelled waters and offshore warm oceanic waters. In the north of the sampling area, the front approached closer to shore before bending strongly offshore in the filament. The structure, arising near 27°N, extended some 150 km as a narrow tongue of water between 21.5 and 22°C, initially northwestwards before turning cyclonically to the south. The filament width around 20 km was defined by strong temperature gradients to both north and south. At its offshore limit, the filament turned cyclonically, surrounding a relatively warm core of diameter >100 km. Other images obtained before and after the survey period

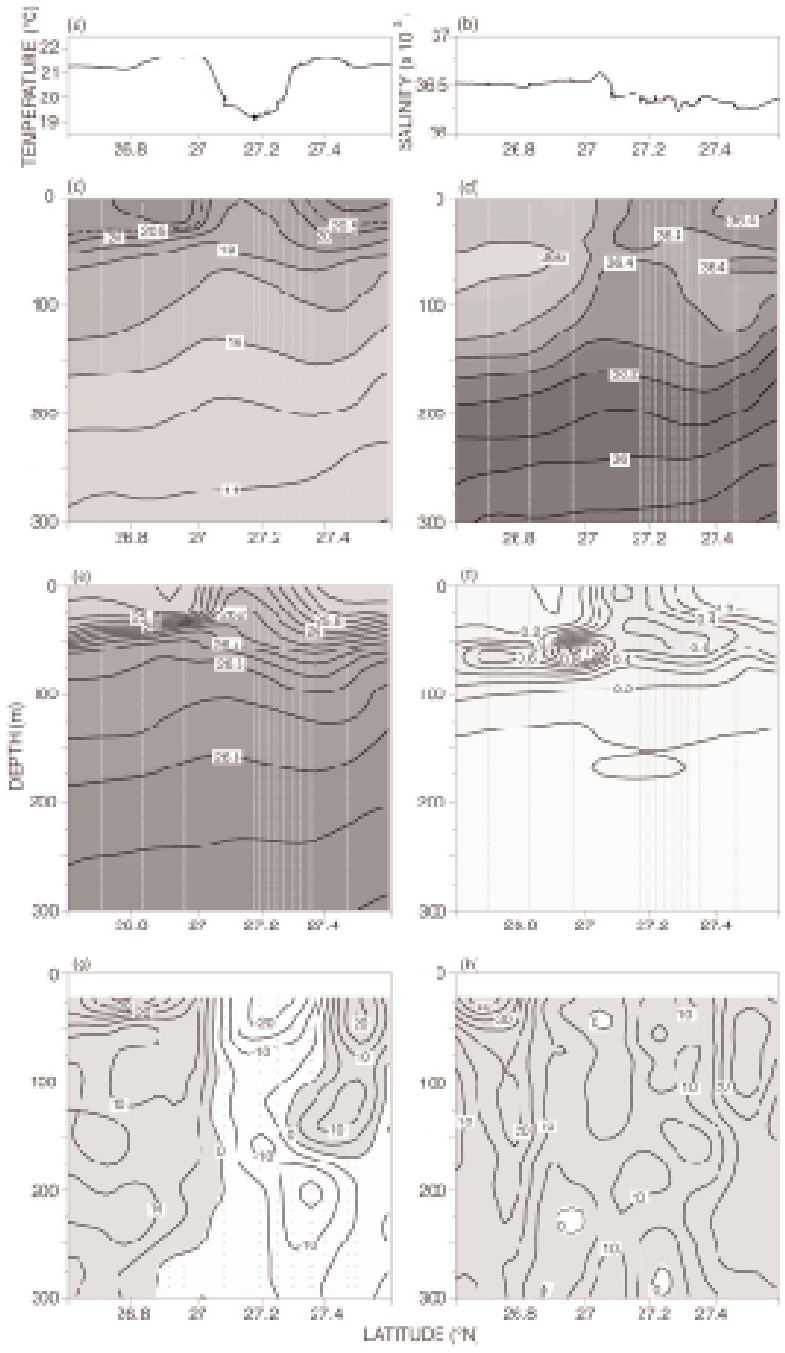

Fig. 2: Profiles of (a) sea surface temperature and (b) salinity and vertical sections of (c) temperature, (d) salinity, (e) density, (f) chlorophyll and (g) onshore and (h) alongshore velocity components for Transect 2

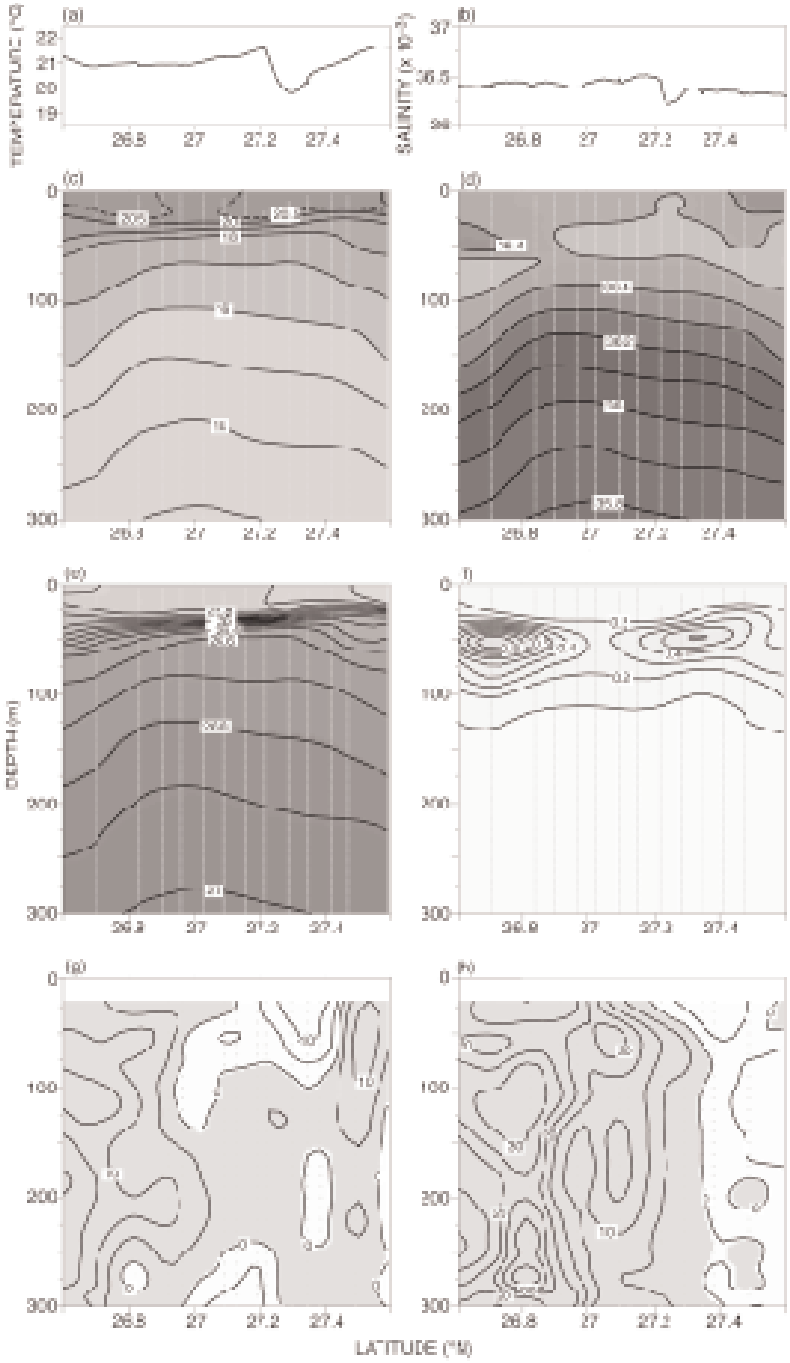

Fig. 3. Profiles of (a) sea surface temperature and (b) salinity and vertical sections of (c) temperature, (d) salinity, (e) density, (f) chlorophyll and (g) onshore and (h) alongshore velocity components for Transect 3

indicated that the principal features of the filament structure persisted over several weeks at least. Low-level cloud prevented acquisition of images during the survey period 11–16 August.

Vertical structure

Transect 1, located nearest the African coast, was mainly inshore of but close to the upwelling front, whereas Transect 2 (Fig. 2), some 30 km farther offshore, clearly crossed the filament structure. Surface temperature values were up to 2°C higher than in the first transect. Thermosalinograph temperature along Transect 2 revealed that filament width was around 28 km while the minimum temperature value in the core of the structure was 2.5°C lower than in surrounding waters. Surface salinity showed little indication of the filament other than increased variability at the edges of the cold anomaly and an increase of ~0.2×10^{-3} from north to south across the feature. The near-surface isotherms sloped steeply up from 50 m to the surface at either side of the filament, which was centred at the surface near 27.15°N. The subsurface isohalines showed strong upwarping in association with the filament, as well as a southward increase of salinity above 150 m depth. Density, dominated by the temperature signal, showed strong horizontal gradients, indicating the presence of significant geostrophic flows related to the filament. Isosurfaces below about 250 m depth did not show any appreciable perturbation associated with the filament. The fluorescence chlorophyll showed a subsurface deep chlorophyll maximum at the base of the pycnocline and low values in the surface layer, except in the filament where there were high values at the surface. A tongue of high chlorophyll extended from the filament at the surface northwards down the sloping isopycnal surfaces.

ADCP velocity data are plotted as components parallel and perpendicular to the sampling transects orientated towards 50°T, so that positive alongshore flow is parallel to the coast in the poleward sense, whereas positive onshore flow is directed towards 140°T. In Transect 2 (Fig. 2), offshore flow coincided with the filament location. Near-surface velocities were 0.25 $m \cdot s^{-1}$ maximum in association with the northern edge of the filament, and the offshore flow extended to depths of at least 200 m. To the south of the filament, the layers above 50 m were flowing shorewards at more than 0.35 $m \cdot s^{-1}$, but at greater depths the flow weakened to about 0.10 $m \cdot s^{-1}$. On the northern side of the filament, onshore flow with a near-surface maximum of 0.20 $m \cdot s^{-1}$ extended down to a depth of 175 m. The alongshore component was almost everywhere polewards, with strongest flow of 0.45 $m \cdot s^{-1}$ near the surface at the southern end of the transect and a weaker maximum at the northern end. There was no indication of convergence in association with the region of the tongue of water high in chlorophyll at the northern edge of the filament. Although the form of the tongue is suggestive of subduction, there is no evidence to substantiate this supposition.

From Transect 2 to Transect 3 (Fig. 3) the filament signal weakened. At the surface, the width of the filament had decreased to about 15 km and the temperature anomaly was less than 2°C, although a clear salinity step and local minimum marked the filament core. The 10-km station spacing did not define the filament in detail, but the upward slope of the isosurfaces towards the feature from both sides was again evident to at least 150 m deep. Fewer isolines broached the sea surface, particularly in chlorophyll, although they may have done so between the two CTD stations straddling the filament. The apparent separation of the near-surface expression of the filament to the north of the strongest disturbance below the pycnocline, where chlorophyll values were also highest, indicates that the filament core lay between CTD casts in this transect.

In Transect 3 (Fig. 3), the offshore flow associated with the filament, located above 100 m depth and between 27°15′ and 27°40′N, was weaker than in Transect 2. Except for a few localized regions, the flow in the rest of Transect 3 was directed onshore. Onshore flow was strongest, less than 0.16 $m \cdot s^{-1}$, at the southern limit of the section. The alongshore component was strongest in the south where values exceeded 0.30 $m \cdot s^{-1}$ directed polewards, but it decreased towards the northern end of the transect, where there was weak equatorward flow.

In the outer three transects, the principal structure revealed was a major doming of the isosurfaces, indicative of strong cyclonic circulation. By Transect 4 (Fig. 4), the filament was detectable in surface profiles as a narrow (~8 km) and weak (~1°C) temperature minimum and salinity step. The 10-km station separation on this transect did not resolve this feature, but it did detect a wider weak near-surface temperature minimum (<20.5°C) near 27°N. This represents remnants of the filament entrained into the cyclonic recirculation evident in Figure 1. Below a depth of 50 m, all isotherms, isohalines and isopycnals indicated a smooth domed structure. The general deep chlorophyll maximum showed two maxima, one close to the narrow surface filament and the other near the wider southern near-surface temperature minimum. The velocity structure indicates that these result from entrainment of the water higher in chlorophyll in the filament around the cyclonic circulation.

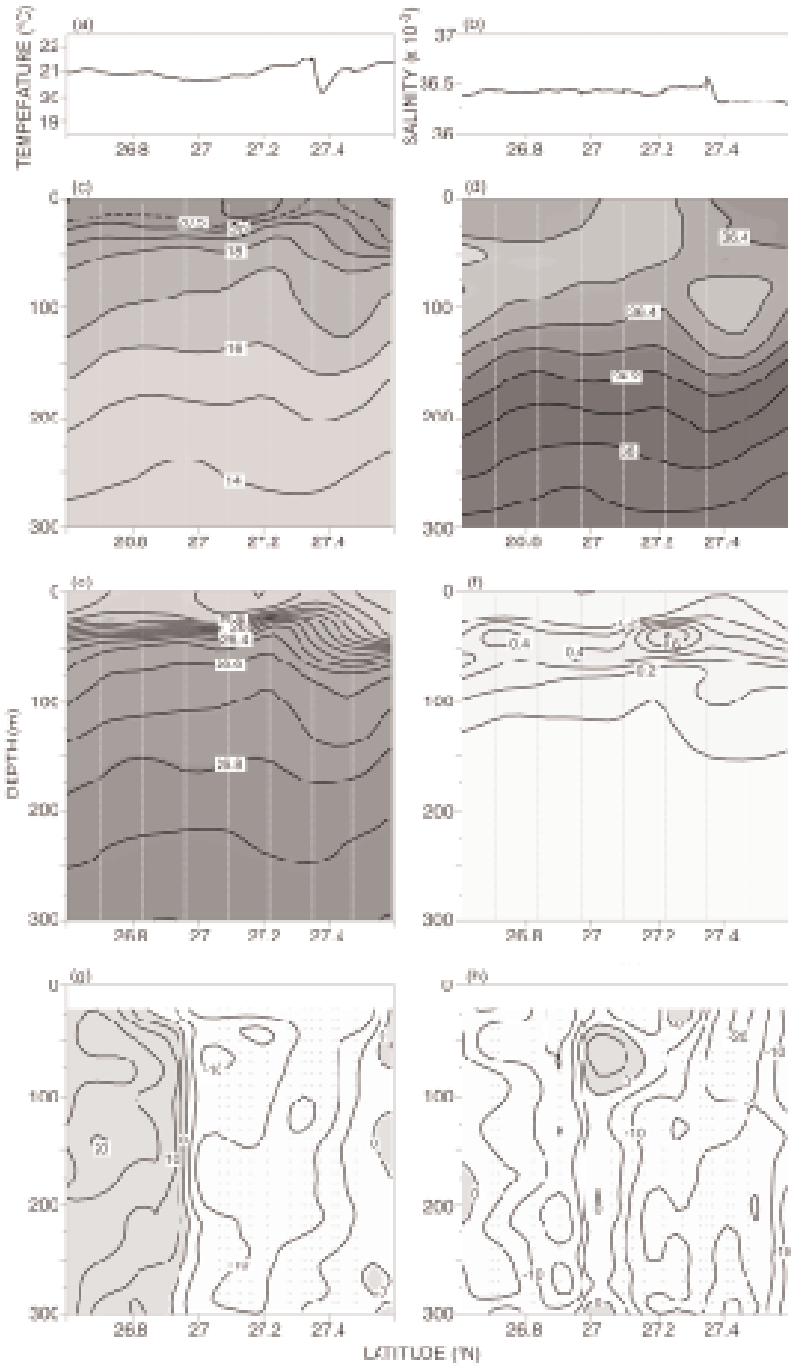

Fig. 4: Profiles of (a) sea surface temperature and (b) salinity and vertical sections of (c) temperature, (d) salinity, (e) density, (f) chlorophyll and (g) on shore and (h) alongshore velocity components for Transect 4

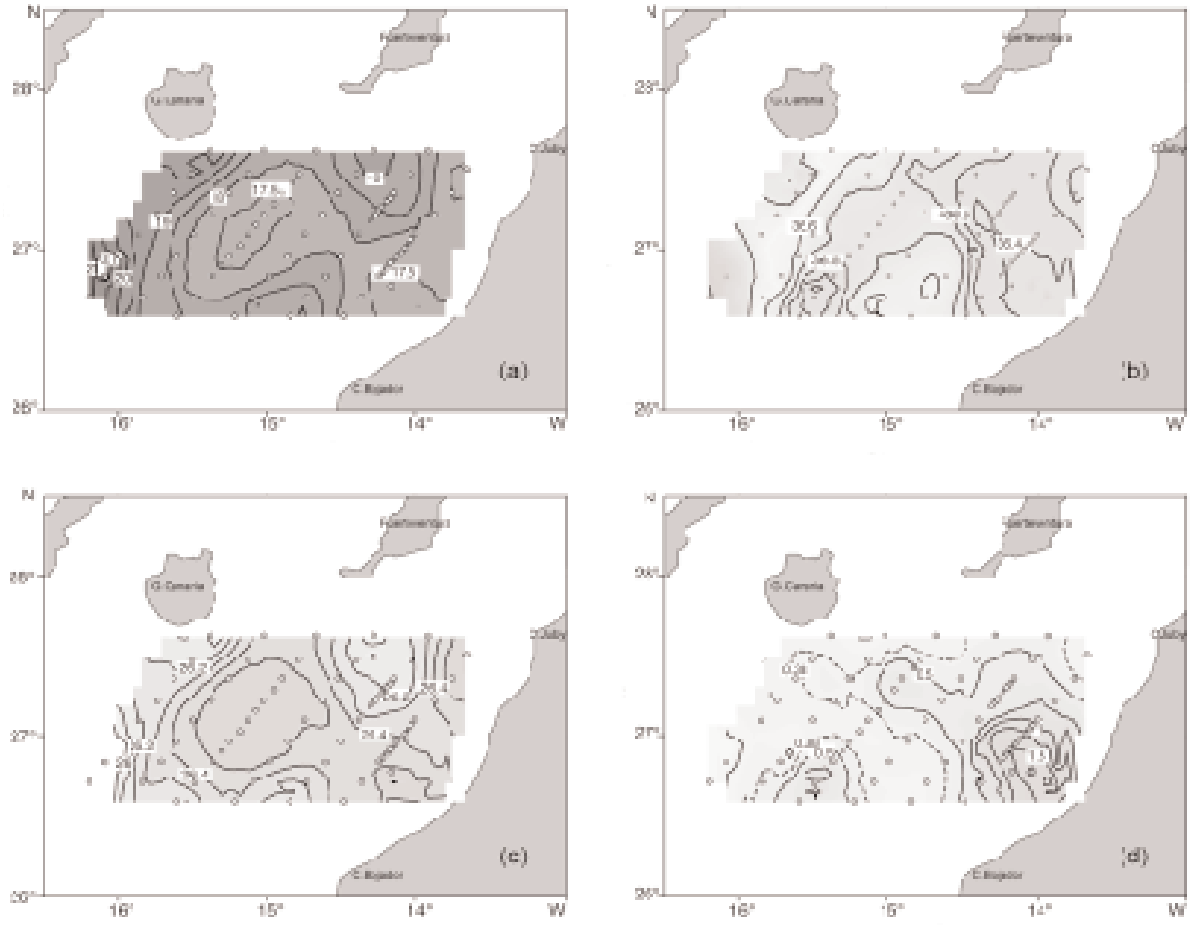

Fig. 5: Maps of (a) temperature, (b) salinity, (c) density anomaly and (d) chlorophyll at 50 m depth

The cross-transect flow was completely offshore north of 27°N and onshore south of there. At the same latitude, the along-transect component decreased to near zero from equatorward values elsewhere throughout the transect.

Both CTD and thermosalinometer datasets revealed that the surface salinity on the north side of the transects was lower than to the south, whereas the filament was marked by a local intermediate or minimum value of salinity. The overall gradient in salinity reflects the general increase of near-surface salinity towards the centre of the subtropical gyre, whereas the filament introduces upwelled coastal water of relatively low salinity into the open ocean waters. To some degree, these characteristics were appreciable in all transects.

Horizontal structure

The horizontal distributions showed the structure associated with the filament to vary as a function of depth. The offshore extension was observed to reach 150 km, as far the Canaries Archipelago, indicating that it may exert an important influence on the islands by introducing cooler, nutrient-rich water into this region of otherwise oligotrophic conditions. At the surface and above the pycnocline (not shown), the filament structure was revealed by the presence of colder water extending offshore in a narrow tongue of temperature between 18.5 and 20°C. The salinity at these depths was more homogeneous, between 36.4 and 36.5 $\times 10^{-3}$ throughout the area, whereas the density structure reflected that of

temperature. The densest, coolest waters were over the continental shelf at the northern and southern limits of the innermost transect, and the filament extended offshore to south of Gran Canaria. Chlorophyll values were 1.6 $mg \cdot m^{-3}$ near-surface close to the coast. Although a tongue of higher chlorophyll marked the filament as it extended offshore, the concentrations decreased quickly to values of only 0.2 $mg \cdot m^{-3}$.

In and below the pycnocline, at a depth of 50 m (Fig. 5), the temperature distribution was quite distinct from the surface distribution seen in Figure 1. It showed a large cool area (<18°C) offshore connected to the waters over the continental shelf by a narrower tongue. The offshore extent of the cooler waters was approximately 150 km. In the centre of the cool area, a minimum of 17.3°C indicated doming of the isotherms. The corresponding salinity map showed less salty water close to the coast, extending in a tongue offshore around the northern periphery of the cool area and following the surface expression of the filament. However, there were lower salinity values spread across the centre of the cool area and a localized minimum in the south of Transect 4. Salinity values generally increased with distance offshore in the tongue and also showed a general increase from north-east to south-west through the area. The density anomaly showed similar structure to temperature, with an offshore high-density region of doming, 100 km in diameter with maximum density anomaly of 26.50 $kg \cdot m^{-3}$. The chlorophyll showed similar tongue-like structure to salinity, with maximum concentrations near the African coast spread out around the northern edge of the cool, dense area, but unlike salinity it did not extend across the centre of the area. In this tongue, values were generally higher than at shallower levels because 50 m corresponds roughly to the deep chlorophyll maximum layer. The isolated maximum of chlorophyll in the south of the survey, corresponding to the salinity minimum, is probably a continuation of the tongue of high chlorophyll under-sampled by the station grid, but it could also reflect patchiness.

At deeper levels, any traces of the filament structure had disappeared, whereas the doming structure in temperature, density, and now salinity persisted. Values in the centre of the offshore cool, dense and less saline area were similar to values at the same depth nearshore affected by the coastal upwelling. Similar doming structure was evident to levels as deep as 600 m.

A map of the ADCP velocity field overlaid on the 0/300 db dynamic topography demonstrates that the filament was intimately related to a large cyclonic eddy in the deeper water off the shelf (Fig. 6). Use of the 300 db level, to include the additional stations inserted between the normal 20-km station spacing, provided more detail than, but was closely similar to, the pattern relative to 1 000 db. The near-surface flow followed the upwelling front and cold filament structure, with southward flow entering the north-east of the study area near the coast, turning strongly offshore to cross Transect 2 at right-angles, and then crossing Transects 3 and 4 farther north before turning south in Transects 5 and 6 around the large eddy structure. In the southern part of the area, the flow swept back towards the coast, some turning north around the eddy and some continuing to the east and showing a tendency to turn equatorwards nearshore. Strongest velocities at this level reached 0.75 $m \cdot s^{-1}$ in the offshore part of the eddy. Flow related to the filament was not detectable deeper than 100 m, but the eddy structure was evident at all levels sampled (down to 350 m). At depths of 125 m and greater, there was an increasing tendency to poleward flow along the continental slope, counter to the surface flow. This poleward flow may be related to the undercurrent found in many locations along the continental slope of the eastern boundary of the North Atlantic Ocean. The undercurrent had a width of less than 75 km between the coast and Transect 2. Maximum undercurrent velocities of about 0.26 $m \cdot s^{-1}$ were located between 26.5 and 27°N at 350 m, in Transect 1.

The vector maps of currents indicated that the cyclonic eddy entrained the near-surface filament around its periphery. The eddy extended at least from Transect 3 to Transect 6, a diameter of 100 km or more, and its centre was located near Transect 4. This structure reached a depth of at least 350 m, as indicated by the deepest ADCP data, and probably 600 m, as shown by doming of the isopycnals.

The velocity structure appeared closely related to the bottom topography in that the eddy was located precisely in the trough south-west of the Fuerteventura-Africa ridge, which has a minimum depth of almost 1 500 m (Fig. 6). As the flow encounters deeper water on crossing the ridge, vortex stretching increases cyclonic vorticity. The main cyclonic eddy then appears topographically generated and therefore is probably a quasi-permanent feature in the general south-westward eastern boundary flow.

A number of smaller structures were seen in the vector maps. For example, part of an anticyclonic eddy appeared close to the African coast, between the northern parts of Transects 1 and 2 (Fig. 6). This structure, of diameter 30 km and maximum depth 125 m, was probably related to the turning offshore of the nearshore current to form the filament. It was observable in the satellite image from 10 August (Fig. 1) between 27.1°W –27.4°N and 14–14.5°W.

The overall depth-averaged (16–300 m) mean

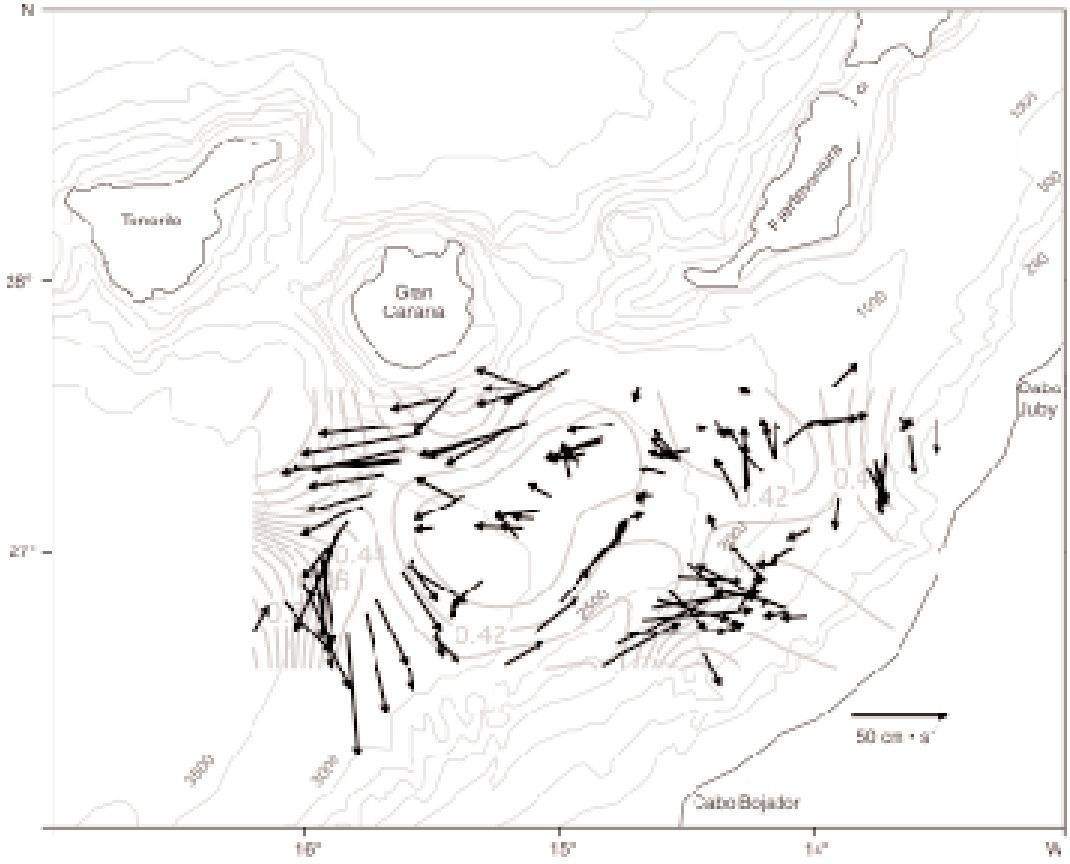

Fig. 6: Map of current velocity vectors 20 m deep overlaid on the dynamic topography of the sea surface with respect to 300 db and the bathymetry. Dynamic height contours are in dynamic metres and isobath depths in metres

northward and eastward velocity components in the filament survey area were −0.025 and −0.037 m·s^{-1} respectively. The overall flow in this region during the sampling period was therefore 0.045 m·s^{-1} towards the south-west, consistent with long-term mean estimates of a weak Canary Current from historical data.

The offshore transport in each transect was calculated by integrating over the cross-sectional area of offshore flow associated with the filament or eddy above 300 m depth. The total transports were 1.2 Sv in Transect 1, 1.1 Sv in Transect 2 and 0.2 Sv in Transect 3. In the eddy structure, the offshore transport increased from Transect 4 to Transect 6, with values of 1.3 Sv and 2.5 Sv respectively. The differences in transport values between the transects were large because some water crossing Transect 2 was exiting the sampled region to the north and re-entering west of Transect 3 as part of the eddy recirculation. Moreover, the flow in the outermost sections was enhanced by additional input entering the area between Gran Canaria, Fuerteventura and the mainland.

The winds during the survey period blew strongly from the north-east with a mean speed of 10 (±4) m·s^{-1}. The corresponding mean Ekman transport was 1.8 m^2·s^{-1}, with maximum values roughly twice as great. Integrating the mean (maximum) value over the 166 km length of the transects provides a total offshore Ekman transport of only 0.3 (maximum 0.6) Sv. This is comparable with the smallest measured offshore transport, in the filament in Transect 3. In that transect the filament was at its narrowest and shallowest, but it was transporting equivalent to almost 70% of the mean Ekman transport over the whole

survey area. Therefore, the filament is potentially a major mechanism for exchange between nearshore and offshore regions. While much of the offshore transport may be re-circulated shoreward, exchanges across the filament boundaries will introduce coastal water characteristics into the oceanic area.

DISCUSSION AND CONCLUSIONS

In relation to the questions posed earlier, the filament has been shown with the hydrographic data to be a superficial structure of limited depth, reaching a maximum depth of only 150 m. The cyclonic eddy extended deeper, showing a strong signal down to at least 350 m. The boundaries of the filament were clearly defined in temperature, salinity and density as sharp fronts in the sections nearer to shore, indicating introduction of a different water mass from the upwelling area. The filament was approximately 150 km long measured to its maximum offshore extent, but distance measured along the filament was greater because it followed a meandering route and wrapped around the cyclonic eddy to return shorewards.

Directly measured currents showed the related velocity structure to consist of a narrow offshore flow which reduced in vertical thickness as the filament extended far from the coast. The cyclonic eddy was clearly an important contributor to the overall structure in the study region. South of the filament structure was an area of onshore return flow, strongest in the cyclonic eddy, but which persisted, albeit reduced in velocity, to approach the coast. The offshore flow in the filament therefore could conceivably be returned to the coast by making a complete loop around the eddy.

The offshore transport was 1 Sv or greater, significantly larger than the Ekman transport integrated over the immediate survey area. Whereas some of this may be recirculated shorewards, exchanges across the filament boundaries can introduce coastal water characteristics into the oceanic area. Similar magnitudes of offshore transport have been reported in filaments off the California coast by Flament *et al.* (1985), Kosro and Huyer (1986) and Ramp *et al.* (1991), on average 1 to 1.5 Sv, and considerably greater than local Ekman transport. Offshore transport in the present filament is comparable to the long-term mean alongshore transport (1.4 Sv) of the Canary Current in the upper 500 m between the African slope and the outer islands, calculated from the historical hydrographic data base (Navarro-Pérez 1996).

The filament appears to correspond neatly with none of the three filament hypotheses proposed for the California Current upwelling by Strub *et al.* (1991). It is not simply a meander of the coastal jet, nor a squirt produced by coastal topography forcing flow offshore, nor attributable to a changing oceanic eddy field. The 100-km diameter cyclonic eddy which dominates the local circulation seems to be permanent. La Violette (1974) reported Airborne Expendable Bathythermograph observations in the region which can be recognized as outlining structure similar to those discussed here. Observations south of Gran Canaria have indicated the influence of an upwelling filament reaching the south-east of the island on different occasions (Arístegui *et al.* 1994, 1997). Sea surface temperature imagery in those papers and more recently (Barton *et al.* in press) shows the filament and eddy structure to recur in many years in essentially the same location.

Examination of the velocity field superimposed on the local bathymetry indicates strong topographic steering. The origin of the eddy is most likely vortex stretching of the flow exiting from the shallower (<1 500 m) channel between the Canary Archipelago and the African coast. The eddy is located over the trough descending south-westwards from the channel. Whenever upwelling is well developed over the continental shelf, the outer boundary of the cold water and associated alongshore current jet may extend far enough offshore to become entrained around the eddy, so producing the filament. Because the existing data represent only one realization of the situation, the variability of the subsurface structure remains undetermined.

The situation contrasts with reports of eddy-filament interaction in the Benguela upwelling region (Shillington *et al.* 1990, Duncombe Rae *et al.* 1992). There, extended filaments can be entrained far offshore around west-drifting oceanic anticyclones arising from the Agulhas retroflection on an intermittent basis. These occurrences resemble the oceanic random eddy-field model of filament production rather than the topographically produced feature at 27°N.

Finally, a major question related to whether filaments are responsible for a net exchange between nearshore and offshore waters is still unresolved. The results off North-West Africa indicate that the filament exports a greater volume than that attributable to the Ekman mechanism, but a large amount is recirculated back towards the coast. Parallel biological studies may be able to show that there is a significant exchange with the surrounding ocean as water travels away from shore in the filament, around the eddy and back again, but for a definitive answer, more detailed physical observations of horizontal exchange processes will be needed.

The main conclusions of the study are listed below.

- A strong filament structure recurs between Cabo Juby and Cabo Bojador, carrying cool water high in chlorophyll offshore from the North-West African coastal upwelling region. It is strongly related to an apparently permanent cyclonic eddy located in the trough south of the ridge between the Canaries and Africa. The coastal upwelling jet becomes entrained around the eddy, transporting with it coastally upwelled water.
- The filament is a narrow (<10–20 km), shallow (<200 m) feature in hydrographic properties, but the associated offshore transport is about 1 Sv, less than the azimuthal transport of the eddy but greater than the 0.3 Sv integrated Ekman transport resulting from the wind. A significant portion of the offshore flow returns to the continental shelf region, presumably continuing south off Cabo Bojador. The extent of mixing between filament and surrounding waters remains to be determined.
- Overall average flow in the survey area was about 0.05 $m \cdot s^{-1}$ to the south-west, similar to estimates from historical data, but the flows are energetic locally. At deeper levels, poleward flow was evident along the slope with speeds 0.25 $m \cdot s^{-1}$ at 200–350 m depth.
- Relatively high values of chlorophyll in the filament are carried around the eddy and may reach close to Gran Canaria. The impact of exchanges between the ocean margin and the open ocean could be a significant factor in enrichment of otherwise oligotrophic waters. The region as a whole is rich in mesoscale structure because of the presence of the Canary Archipelago. Island lee regions and eddies of both signs spun off from the islands contribute to vertical and horizontal exchanges. Work to study the interaction between these features and filaments is continuing.

ACKNOWLEDGEMENTS

This work was partially supported by the European Commission under MAST I project 0031. Fieldwork was financed by the Comisión Interministerial de Ciencia y Tecnología of Spain. We thank our many colleagues in the project for their help and advice. E. Navarro-Pérez was supported by European Union studentships CEC/910792 and 913012.

LITERATURE CITED

ALLEN, J. S., WALSTAD, L. J. and P. A. NEWBERGER 1991 — Dynamics of the coastal transition zone jet. 2. Nonlinear finite amplitude behavior. *J. geophys. Res.* **96**(C8): 14995–15016.

ARÍSTEGUI, J., SANGRÁ, P., HERNÁNDEZ-LEÓN, S., CANTÓN, M., HERNÁNDEZ-GUERRA, A. and J. L. KERLING 1994 — Island-induced eddies in the Canary Islands. *Deep-Sea Res.* **41**(10): 1509–1525.

ARÍSTEGUI, J., TETT, P., HERNÁNDEZ-GUERRA, P., BASTERRETXEA, G., MONTERO, M. F., WILD, K., SANGRÁ, P., HERNÁNDEZ-LEÓN, S., CANTÓN, M, GARCÍA-BRAUN, J. A., PACHECO, M. and E. D. BARTON 1997 — The influence of island-generated eddies on chlorophyll distribution: a case study of mesoscale variation around Gran Canaria. *Deep-Sea Res.* **44**(1): 71–96.

BARTON, E. D., ARÍSTEGUI, J., TETT, P., CANTÓN, M., GARCÍA-BRAUN, J. A., HERNÁNDEZ-LEÓN, S., NYKJAER, L., ALMEIDA, C., ALMUNIA, J., BALLESTEROS, G., BASTERRETXEA, G., ESCANEZ, J., GARCIA-WEILL, L., HERNÁNDEZ-GUERRA, A., LOPEZ-LAATZEN, F., MOLINA, R., MONTERO, M. F., NAVARRO-PEREZ, E., RODRIGUEZ, J. M., VAN LENNING, K., VELEZ, H. and K. WILD (in press) — The transition zone of the Canary Current upwelling region. *Prog. Oceanogr.*

BRINK, K. H. and T. J. COWLES 1991 — The Coastal Transition Zone program. *J. geophys. Res.* **96**(C8): 14637–14647.

DUNCOMBE RAE, C. M., SHILLINGTON, F. A., AGENBAG, J. J., TAUNTON-CLARK, J. and M. L. GRÜNDLINGH 1992 — An Agulhas ring in the South Atlantic Ocean and its interaction with the Benguela upwelling frontal system. *Deep-Sea Res.* **39**(11A/12A): 2009–2027.

FLAMENT, P., ARMI, L. and L. WASHBURN 1985 — The evolving structure of an upwelling filament. *J. geophys. Res.* **90**(C6): 11765–11778.

HAIDVOGEL, D. B., BECKMANN, A. and K. S. HEDSTRÖM 1991 — Dynamical simulations of filament formation and evolution in the coastal transition zone. *J. geophys. Res.* **96**(C8): 15017–15040.

HAYNES, R., BARTON, E. D. and I. PILLING 1993 — Development, persistence, and variability of upwelling filaments off the Atlantic coast of the Iberian Peninsula. *J. geophys. Res.* **98**(C12): 22681–22692.

HERNÁNDEZ-GUERRA, A. 1990 — Estructuras oceanográficas observadas en las aguas que rodean las Islas Canarias mediante escenas de los sensores AVHRR y CZCS. Ph.D. thesis, Universidad de Las Palmas de Gran Canaria, Spain: 198 pp.

HUTHNANCE, J. M. and P. G. BAINES 1982 — Tidal currents in the north-west African upwelling region. *Deep-Sea Res.* **29**(3A): 285–306.

HUYER, A., KOSRO, P. M., FLEISCHBEIN, J., RAMP, S. R., STANTON, T., WASHBURN, L., CHAVEZ, F. P., COWLES, T. J., PIERCE, S. D. and R. L. SMITH 1991 — Currents and water masses of the coastal transition zone off northern California, June to August 1988. *J. geophys. Res.* **96**(C8): 14809–14831.

IKEDA, M. and W. J. EMERY 1984 — Satellite observations and modelling of meanders in the California Current system off Oregon and northern California. *J. phys. Oceanogr.* **14**: 1434–1450.

KOSRO, P. M. and A. HUYER 1986 — CTD and velocity surveys of seaward jets off northern California, July 1981 and 1982. *J. geophys. Res.* **91**(C6): 7680–7690.

LA VIOLETTE, P. E. 1974 — A satellite-aircraft thermal study of the upwelled waters off Spanish Sahara. *J. phys. Oceanogr.* **4**: 676–684.

LUTJEHARMS, J. R. E. and P. L. STOCKTON 1987 — Kinematics of the upwelling front off southern Africa. In *The Benguela and Comparable Ecosystems*. Payne, A. I. L., Gulland, J. A. and K. H. Brink (Eds). *S. Afr. J. mar. Sci.* **5**: 35–49.

McCREARY, J. P., FUKAMACHI, Y. and P. K. KUNDU 1991 — A numerical investigation of jets and eddies near an eastern ocean boundary. *J. geophys. Res.* **96**(C2): 2515–2534.

MOOERS, C. N. K. and A. R. ROBINSON 1984 — Turbulent jets and eddies in the California Current and inferred cross-shore transports. *Science, N.Y.* **223**(4631): 51–53.

NARIMOUSA, S. and T. MAXWORTHY 1986 — Effects of a discontinuous surface stress on a model of coastal upwelling. *J. phys. Oceanogr.* **16**: 2071–2083.

NAVARRO-PÉREZ, E. 1996 — Physical oceanography of the Canary Current: short term, seasonal and interannual variability. Ph.D. thesis, University of Wales, Bangor: 230 pp.

NAVARRO-PÉREZ, E. and E. D. BARTON 1995 — BIO Hespérides cruise report: Acoustic Doppler Current Fields. European Coastal Transition Zone Islas Canarias. MAST Project Report 0031–19; University College of North Wales, Bangor: 71 pp. (mimeo).

NAVARRO-PÉREZ, E., VELEZ-MUÑOZ, H. S. and K. A. WILD 1994 — BIO Hespérides Cruise 9308, cruise report: hydrographic fields. European Coastal Transition Zone Islas Canarias. MAST Project Report 0031–16; University College of North Wales, Bangor: 150 pp. (mimeo).

PACHECO, M and A. HERNÁNDEZ-GUERRA 1995 — Hespérides Cruise Report: thermosalinometer and Fluorometer Data. European Coastal Transition Zone Islas Canarias MAST Project Report 0031–20; University College of North Wales, Bangor: 21 pp. (mimeo).

PIERCE, S. D., ALLEN, J. S and L. J. WALSTAD 1991 — Dynamics of the coastal transition zone jet. 1. Linear stability analysis. *J. geophys. Res.* **96**(C8): 14979–14993.

RAMP, R. S., JESSEN, P. F., BRINK, K. H., NIILER, P. P., DAGGETT, F. L. and J. S. BEST 1991 — The physical structure of cold filaments near Point Arena, California, during June 1987. *J. geophys. Res.* **96**(C8): 14859–14883.

RIENECKER, M. M. and C. N. K. MOOERS 1989 — Mesoscale eddies, jets, and fronts off Point Arena, California, July 1986. *J. geophys. Res.* **94**(C9): 12555–12569.

SHILLINGTON, F. A., PETERSON, W. T., HUTCHINGS, L., PROBYN, T. A., WALDRON, H. N. and J. J. AGENBAG 1990 — A cool upwelling filament off Namibia, southwest Africa: preliminary measurements of physical and biological properties. *Deep-Sea Res.* **37**(11A): 1753–1772.

STRUB, P. T., KOSRO, P. M., HUYER, A. J., JAMES, C., WALSTAD, L. J., SMITH, R. L., BARTH, J. A., HOOD, R. R., ABBOTT, M. R., BRINK, K. H., HAYWARD, T. L., NIILER, P. P., SWENSON, M. S., DEWEY, R. K., CHAVEZ, F., RAMP, S. R., BATTEEN, M. L., HANEY, R. L., MACKAS, D. L., WASHBURN, L., KADKO, D. C., BARBER, R. T. and D. B. HAIDVOGEL 1991 — The nature of the cold filaments in the California Current system. *J. geophys. Res.* **96**(C8): 14743–14768.

VAN CAMP, L., NYKJAER, L., MITTELSTAEDT, E. and P. SCHLITTENHARDT 1991 — Upwelling and boundary circulation off Northwest Africa as depicted by infrared and visible satellite observations. *Prog. Oceanogr.* **26**(4): 357–402.